

# DETReg: Unsupervised Pretraining with Region Priors for Object Detection

Amir Bar<sup>1</sup>, Xin Wang<sup>5</sup>, Vadim Kantorov<sup>1</sup>, Colorado J Reed<sup>2</sup>, Roei Herzig<sup>1</sup>,  
Gal Chechik<sup>3,4</sup>, Anna Rohrbach<sup>2</sup>, Trevor Darrell<sup>2</sup>, Amir Globerson<sup>1</sup>

<sup>1</sup> Tel-Aviv University   <sup>2</sup> Berkeley AI Research   <sup>3</sup> NVIDIA   <sup>4</sup> Bar-Ilan University   <sup>5</sup> Microsoft Research  
amir.bar@cs.tau.ac.il

## Abstract

Recent self-supervised pretraining methods for object detection largely focus on pretraining the backbone of the object detector, neglecting key parts of detection architecture. Instead, we introduce DETReg, a new self-supervised method that pretrains the entire object detection network, including the object localization and embedding components. During pretraining, DETReg predicts object localizations to match the localizations from an unsupervised region proposal generator and simultaneously aligns the corresponding feature embeddings with embeddings from a self-supervised image encoder. We implement DETReg using the DETR family of detectors and show that it improves over competitive baselines when finetuned on COCO, PASCAL VOC, and Airbus Ship benchmarks. In low-data regimes DETReg achieves improved performance, e.g., when training with only 1% of the labels and in the few-shot learning settings.<sup>1</sup>

## 1. Introduction

Object detection is a key task in computer vision, yet it largely relies on the availability of human-annotated training datasets. Building such datasets is not only costly but sometimes infeasible for privacy-sensitive applications such as medical imaging or personal photos [46, 68]. Fortunately, recent advancements in self-supervised representation learning have substantially reduced the amount of labeled data needed for a variety of applications, including object detection [6, 11, 26, 27].

Despite this recent progress, current approaches are limited in their ability to learn good representations for object detection because they do not pretrain the entire object detection network, specifically the localization and region embedding components. Most recent works (e.g., SwAV [6], ReSim [62], InsLoc [67]) follow the same *pre-training playbook* for the detection network as a super-

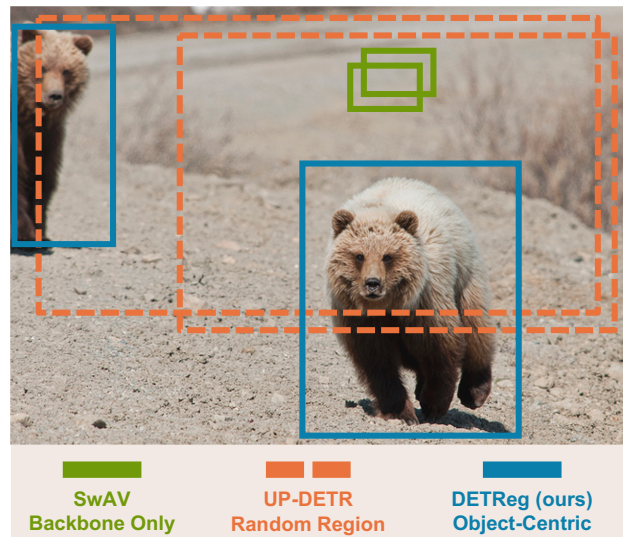


Figure 1. **Top class-agnostic object detections after pretraining.** Self-supervised pretraining methods, such as SwAV [6], pretrain only the detector’s backbone, so the object localizations following the pretraining stage solely depend on the random initialization of the localization components (green). UP-DETR [16] pretrains the entire detection network, but since its pretraining operates by re-identifying random regions, it does not specialize in localizing objects after the pretraining (orange dashes). Our model, DETReg, pretrains the entire detection network using object-centric pretraining, and following the pretraining stage can localize objects (blue).

vised image-classification-based pretraining, where only the CNN backbone can be initialized from the pretrained model. While the recent UP-DETR [16] method pretrains a full detection architecture, it still does not localize objects within the image, but rather random image regions.

In this work, we present a model for Detection with Transformers using Region priors (DETReg), which unlike existing pretraining methods, learns to both localize and encode objects simultaneously in the unsupervised pretraining stage – see Figure 1. DETReg involves two object-centric and

<sup>1</sup>Code: <https://www.amirbar.net/detreg/>.

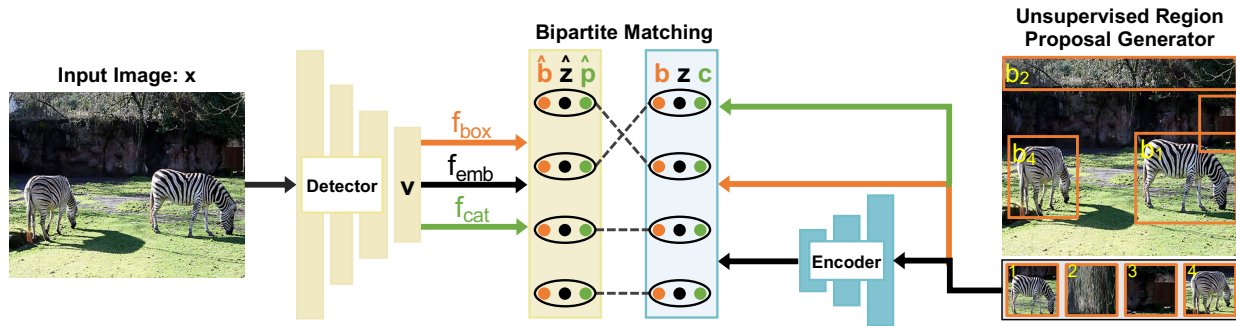


Figure 2. The **DETReg** model and pretext tasks. Given embeddings  $v$  from image  $x$ , we use the DETR family of detectors [5, 71] to predict region proposals ( $f_{box}(v) = \hat{b}$ ), associated object embeddings ( $f_{emb}(v) = \hat{z}$ ), and object scores ( $f_{cat}(v) = \hat{p}$ ). Pseudo ground-truth region proposals labels ( $b$ ) can be generated by existing unsupervised region proposal methods like [54, 59], and pseudo ground-truth object embeddings ( $z$ ) can be generated via existing self-supervised approaches like [6, 27], where the object score  $c$  is always 1 for these proposals. Predictions are assigned to pseudo labels via Bipartite Matching, and unmatched predictions are assigned with padded proposals with  $c = 0$ .

category-agnostic pretraining tasks: an *Object Localization Task* to localize objects, and an *Object Embedding Task* to encode an object’s visual properties. Taken together, these tasks pretrain the entire detection network – see Figure 2 for an overview. A final object classification head can then be finetuned with a small number of labels yielding better performance than existing methods.

DETReg’s object localization task uses simple region proposal methods for class-agnostic bounding-box supervision [3, 3, 14, 15, 54]. These methods require little or no training data and can produce region proposals at a high recall. For example, Selective Search [54], the region proposal method we adopt in DETReg, uses object cues such as continuity in color, hierarchy, and edges to extract object proposals. DETReg builds upon these region priors to learn a class-agnostic detector during pretraining.

DETReg’s object embedding task aims to predict the embeddings of a separate self-supervised image encoder evaluated on object regions. Self-supervised image encoders, e.g., SwAV [6], learn transformation-invariant embeddings, so training the detector to predict these values distills the learned invariances into the detector’s embeddings. Thus, the object embedding head learns representations that are robust to transformations such as translation or image cropping.

We conduct an extensive evaluation of DETReg on standard object detection benchmarks like MS COCO [41] and PASCAL VOC [18], and on an aerial images dataset, Airbus Ship Detection [1]. We find that DETReg improves the performance using two state-of-the-art base architectures compared to challenging baselines, especially when small amounts of annotated data are available.

Quantitatively, DETReg improves over a backbone-only image-classification pretraining baseline by 4 AP points on PASCAL VOC, 1.6 AP points on MS COCO, and 1.2 AP

points on Airbus Ship Detection. Additionally, DETReg outperforms pretraining baselines in semi-supervised learning when using 1% to 10% of data, and on 10 and 30 shot. Taken together, these results indicate that pretraining an entire detection network, including region proposal prediction and embedding components, is beneficial and that our specific DETReg model realizes new SOTA performance by taking advantage of this object-centric self-supervised pretraining.

## 2. Related Work

**Self-supervised pretraining.** Recent work [6, 10, 13, 22, 25, 27, 28, 31, 43] has shown that self-supervised pretraining can generate powerful representations for transfer learning, even outperforming its supervised counterparts on challenging vision benchmarks [10, 61]. The learned representations transfer well to image classification but the improvement is less significant for instance-level tasks, such as object detection and instance segmentation [27, 29, 48, 70].

More recently, a number of works [31, 51, 62, 64] focused on learning backbones that can transfer to object detection. In contrast to these works, we pretrain the entire detection network. As we show, pretraining the backbone with an image-patch-based task does not necessarily empower the model to learn *what and where* an object is, and adding weak supervision from the region priors proves beneficial.

Our approach is also different from semi-supervised object detection approaches [34, 42, 53, 65] and few-shot detection approaches [9, 12, 19, 20, 35, 36, 39, 56, 59, 60, 63, 66, 69] as we initialize the detector from a pretrained DETReg model without further modifying the architecture. Therefore, these approaches can be viewed as complementary to DETReg.

**End-to-end object detection.** Detection with transformers (DETR) [5] builds the first fully end-to-end object de-

tector and eliminates the need for components such as anchor generation and non-maximum suppression (NMS) post-processing. This model has quickly gained traction in the machine vision community. However, the original DETR suffers from slow convergence and limited sample efficiency. Deformable DETR [71] introduced a deformable attention module to attend to a sparsely sampled small set of prominent key elements, and achieved better performance compared to DETR with reduced training epochs. We therefore use Deformable DETR as our base detection architecture.

Both DETR and Deformable DETR adopt the supervised pretrained backbone (ResNet [30]) on ImageNet. UP-DETR [16] pretrains DETR in a self-supervised way by detecting and reconstructing the random patches from the input image. Instead, we additionally adopt region priors from unsupervised region proposal algorithms to provide weak supervision for pretraining, which has an explicit notion of *objects* rather than the random patches used by UP-DETR.

**Region proposals.** A rich study of region proposals methods exists in the object detection literature [2, 3, 8, 15, 17, 37, 55, 72]. Grouping based method, Selective Search [55], and window scoring based approach, Objectness [2] are two early and well known proposal methods, which have been widely adopted and supported in major software libraries (e.g., OpenCV [4]). Selective Search greedily merges superpixels to generate proposals. Objectness relies on visual cues such as multi-scale saliency, color contrast, edge density and superpixel straddling to identify likely regions.

While the field has largely shifted to learning-based approaches, the key benefit of these models is that they require little or no training data, and can produce region proposals at a high recall [3, 3, 14, 15, 54]. This provides a cheap, albeit noisy, source of supervision. Hosang *et al.* [32, 33] offer a comprehensive analysis over the various region proposals methods, and Selective Search is among the top performing approaches in terms of recall. Here, we seek weak supervision from the region proposals generated by Selective Search, which has been widely adopted and proven successful in the well-known detectors such as R-CNN [24] and Fast R-CNN [23]. However, our approach is not limited to Selective Search and can employ other proposal methods.

### 3. DETReg

DETReg is a self-supervised method to fully pretrain object detectors, including their region localization and embedding components. At a high level, DETReg operates by predicting object localizations that match those from an unsupervised region proposal generator, while simultaneously aligning the corresponding feature embeddings with embeddings from a self-supervised image encoder, see Figure 2.

The key idea underlying DETReg is to formulate pretext tasks that are similar to the tasks performed during super-

vised object detection, so that improved pretraining transfers to the object detector. We built DETReg based on the DETR family of detectors [5, 71] due to their implementation simplicity and performance, though other architectures can easily plug into DETReg. Next, we review DETR, and in the following subsections, we present the object localization and embedding pretext tasks that form the core of DETReg.

**DETR summary:** DETR detects up to  $N$  objects in an image by iteratively applying attention and feed-forward layers over  $N$  object query vectors of a transformer decoder and over the input image features. The last layer of the decoder results in  $N$  image-dependent query embeddings that are used to predict bounding box coordinates and object categories. Formally, consider an input image  $x \in \mathbb{R}^{H \times W \times 3}$ . DETR uses  $x$  to calculate  $N$  image-dependent query embeddings  $v_1, \dots, v_N$  with  $v_i \in \mathbb{R}^d$ . This is achieved by passing the image through a backbone, followed by a transformer, and processing of the query vectors [5]. Then, two prediction heads are applied to  $v_i$ . The first,  $f_{box} : \mathbb{R}^d \rightarrow \mathbb{R}^4$ , predicts the bounding boxes. The second,  $f_{cat} : \mathbb{R}^d \rightarrow \mathbb{R}^L$ , outputs a distribution over  $L$  object categories, including a background “no object” category.

#### 3.1. Object Localization Task

DETReg’s object localization pretraining task uses simple region proposal methods for class-agnostic bounding-box supervision (see the orange arrows in Figure 2). We use the output from these methods as they require limited or no training data and can produce region proposals at a high recall [3, 14, 15, 54]. We use Selective Search [54] as the primary region proposal method for training DETReg as it is widely available in off-the-shelf computer vision libraries and requires no training data. Selective Search uses object cues such as continuity in color and edges to extract object proposals, and DETReg further builds upon these region priors to learn a class-agnostic detector.

Region proposal methods take an image and produce a large set of region proposals at a high recall rate, where some of the regions are likely to contain objects. However, they have low precision and do not output category information, see [32, 33]. Since the content of non-object boxes tends to be more variable than of object boxes, we expect that deep models can be trained to recognize the visual properties of objects even when given noisy labels.

Thus, the *Object Localization* pretraining task takes a set of  $M$  boxes  $b_1, \dots, b_M$  (where  $b_i \in \mathbb{R}^4$ ) output by an unsupervised region proposal method and optimizes a loss that minimizes the difference between the detector box predictions (the output of the  $f_{box}$  MLP) and these  $M$  boxes. Similar to DETR, the loss involves matching the predicted boxes and these  $M$  boxes, a process we detail in Section 3.3.

Common region proposal methods attempt to sort the region proposals such that proposals that are more likely to

be objects appear first, however, the number of proposals is typically large, and the ranking is not precise. Therefore, we explore methods to choose the best regions to use during training. We consider three policies for selecting boxes:

**Top-K** uses the top- $K$  proposals from the algorithm.

**Random-K** uses  $K$  random proposals, which may yield lower quality proposals but encourages exploration.

**Importance Sampling** relies on the region proposal method ranking but also encourages more diverse proposals. Formally, let  $\mathbf{b}_1, \dots, \mathbf{b}_n$  be a set of  $n$  sorted region proposals, where the  $\mathbf{b}_i$  has rank  $i$ . Let  $X_i$  be a random variable indicating whether we will output the  $\mathbf{b}_i$ . We assign the sampling probability for  $X_i$  to be:  $Pr(X_i = 1) \propto -\log(i/n)$ . To determine if a box should be included, we randomly sample from its respective distribution.

### 3.2. Object Embedding Task

In the supervised training of object detectors, every box is associated with a class category of the object, which is not available in an unsupervised setting. Therefore, to learn a strong object embedding, we encode each box region  $\mathbf{b}_i$  via a separate encoder network and obtain embeddings  $\mathbf{z}_i$  that are used as a target for the DETReg embeddings  $\hat{\mathbf{z}}_i$  (see the black arrows in Figure 2).

The separate encoding network that produces  $\mathbf{z}_i$  could be jointly trained by following similar bootstrapping techniques from works such as BYOL [26] or DINO [7]. However, for training stability and to reduce the convergence time, we leverage a pretrained, self-supervised model whose embeddings are invariant to many image transformations, e.g. blurring and color distortions. Here we primarily use a SwAV [6] pretrained model as it is one of the strongest performing methods for pretraining image classifiers and has readily available code and pretrained models.

To predict a corresponding object embedding  $\hat{\mathbf{z}}_i$  in the detector, we introduce an additional MLP  $f_{emb} : \mathbb{R}^d \rightarrow \mathbb{R}^d$  that predicts the object embedding  $\hat{\mathbf{z}}_i$  from the corresponding DETR query embedding,  $\mathbf{v}_i$ . This encourages  $\mathbf{v}_i$  to capture the information that is useful for category prediction. The loss is the  $L_1$  loss between  $\hat{\mathbf{z}}_i$  and  $\mathbf{z}_i$ .

### 3.3. DETReg Pretraining

Here, we formally describe how DETReg optimizes the localization and embedding tasks during pretraining. Assume that our region proposal method returns  $M$  object proposals which are used to generate  $M$  bounding boxes  $\mathbf{b}_i$  and object descriptors  $\mathbf{z}_i$  for  $i \in \{1, \dots, M\}$ , and let  $y_i = (\mathbf{b}_i, \mathbf{z}_i)$  with  $y = \{y_i\}_{i=1}^M$ . DETReg is trained such that its  $N$  outputs align with  $y$ .

Let  $\mathbf{v}_1, \dots, \mathbf{v}_K$  denote the image-dependent query embeddings calculated by DETR (i.e., the output of the last layer of the DETR decoder). DETReg has three prediction

heads:  $f_{box}$  which outputs predicted bounding boxes,  $f_{cat}$  which predicts if the box is object or background, and  $f_{emb}$  which reconstructs the object embedding descriptor. Denote these outputs as:  $\hat{\mathbf{b}}_i = f_{box}(\mathbf{v}_i)$ ,  $\hat{\mathbf{z}}_i = f_{emb}(\mathbf{v}_i)$ ,  $\hat{\mathbf{p}}_i = f_{cat}(\mathbf{v}_i)$ , and define  $\hat{y}_i = (\hat{\mathbf{b}}_i, \hat{\mathbf{z}}_i, \hat{\mathbf{p}}_i)$  and  $\hat{y} = \{\hat{y}_i\}_{i=1}^N$ .

Following DETR training, we assume that the number of DETR queries  $N$  is larger than  $M$ , so we pad  $y$  to obtain  $N$  tuples, and assign a label  $c_i \in \{0, 1\}$  to each box in  $y$  to indicate whether it is a region proposal ( $c_i = 1$ ) or padded proposal ( $c_i = 0$ ); see the green arrows in Figure 2. With the DETR family of detectors [5, 71], there are no assumptions on the order of the labels or the predictions and therefore we first match the objects of  $y$  to the ones in  $\hat{y}$  via the Hungarian bipartite matching algorithm [38]. Specifically, we find the permutation  $\sigma$  that minimizes the optimal matching cost between  $y$  and  $\hat{y}$ :

$$\sigma = \arg \min_{\sigma \in \Sigma_N} \sum_i^N L_{match}(y_i, \hat{y}_{\sigma(i)}) \quad (1)$$

Where  $L_{match}$  is the pairwise matching cost matrix as defined in [5, 71] and  $\Sigma_N$  is the set of all permutations over  $\{1 \dots N\}$ . Using the optimal  $\sigma$ , we define the loss as:

$$\begin{aligned} L(y, \hat{y}) = & \sum_{i=1}^N \lambda_f L_{class}(c_i, \hat{\mathbf{p}}_{\sigma(i)}) + \\ & \mathbb{1}_{\{c_i \neq 0\}} (\lambda_b L_{box}(\mathbf{b}_i, \hat{\mathbf{b}}_{\sigma(i)}) + \\ & \lambda_e L_{emb}(\mathbf{z}_i, \hat{\mathbf{z}}_{\sigma(i)})) \end{aligned} \quad (2)$$

Where  $L_{class}$  is the class loss, that can be implemented via Cross Entropy Loss or Focal Loss [40], and  $L_{box}$  is based on the the  $L_1$  loss and the Generalized Intersection Over Union (GIoU) loss [50]. Finally, we define  $L_{emb}$  to be the  $L_1$  loss:

$$L_{emb}(\mathbf{z}_i, \mathbf{z}_j) = \|\mathbf{z}_i - \hat{\mathbf{z}}_j\|_1 \quad (3)$$

## 4. Experiments

We first describe the implementation details and datasets used for our experimentation. We then report how DETReg performs on the object detection tasks when finetuned on full and low-data regimes, including few-shot learning, and semi-supervised learning. Finally, we conclude with ablations, analyses, and visualizations from DETReg.

**Implementation.** Based on the ablations presented in Section 4.5, the default experiment settings are as follows (see the Suppl. for all details). We initialize the ResNet50 backbone of DETReg with SwAV [6], which was pretrained with multi-crop views for 800 epochs on IN1K, and fix it throughout the pretraining stage. In the object embedding branch,  $f_{emb}$  and  $f_{box}$  are MLPs with 2 hidden layers of size 256 followed by a ReLU [44] nonlinearity. The output sizes of  $f_{emb}$  and  $f_{box}$  are 512 and 4.  $f_{cat}$  is implemented as a single fully-connected layer with 2 outputs. Unless otherwise

Pretraining	Detector	Epochs	AP	AP <sub>50</sub>	AP <sub>75</sub>
Supervised	DETR	150	39.5	60.3	41.4
SwAV [6]			39.7	60.3	41.7
UP-DETR			40.5	60.8	42.6
<b>DETReg</b>			<b>41.9<sup>+1.4</sup></b>	<b>61.9<sup>+1.1</sup></b>	<b>44.1<sup>+1.5</sup></b>
Supervised	DETR	300	40.8	61.2	42.9
SwAV [6]			42.1	63.1	44.5
UP-DETR			42.8	63.0	45.3
<b>DETReg</b>			<b>43.7<sup>+0.9</sup></b>	<b>63.7<sup>+0.7</sup></b>	<b>46.6<sup>+1.3</sup></b>
Supervised	DDETR	50	44.5	63.6	48.7
SwAV [6]			45.2	64.0	49.5
UP-DETR			44.7	63.7	48.6
<b>DETReg</b>			<b>45.5<sup>+0.8</sup></b>	<b>64.1<sup>+0.4</sup></b>	<b>49.9<sup>+1.3</sup></b>

Table 1. **Object detection results when trained on MS COCO train2017 and evaluated on val2017.** Both DETReg and UP-DETR are pretrained on IN1K under comparable settings, while supervised and SwAV only pretrain the backbone of the object detector. We explore both the DETR and Deformable DETR (DDETR) architectures; for compatibility with prior work, we finetuned the DETR for 150/300 epochs and DDETR for 50 epochs.

noted, we use the DETReg Top-K region selection variant (see Section 3.1) and set  $K = 30$  proposals per-image.

**Datasets.** We use the following datasets: **ImageNet ILSRVC 2012** (IN1K) dataset contains 1.2M images with 1000 class categories. As done in prior work [6, 10, 62, 64], we use the unlabeled IN1K data for pretraining. Similar to other works [27, 28, 62], we use a subset of IN1K called **IN100** that contains  $\sim 125$ K images and 100 class categories for several ablation studies. **MS COCO** [41] is a popular object detection benchmark that contains 121K labeled images, where objects from 80 object categories are annotated with bounding boxes. **PASCAL VOC** [18] contains  $\sim 20$ K natural images where the objects from 21 classes are annotated. To explore a dataset with different visual properties than the typical object-centric benchmarks, we use the **Airbus Ship Detection** dataset [1], which contains  $\sim 231$ K satellite images annotated with bounding boxes of ships. Following [45], we convert the segmentation masks to bounding boxes and use a 42.5K image subset, with 3K test/val splits.

#### 4.1. Object Detection in Full Data Regimes

These experiments test how well DETReg performs when a fully annotated dataset is available for finetuning.

**Pretraining.** We pretrain two variants of DETReg based on DETR [5] and Deformable DETR [71] detectors for 5 and 60 epochs on IN1K and IN100, respectively, where the pretraining schedules are set by proportionally adjusting the schedules used in UP-DETR to equate to the more efficient Deformable DETR schedules [71].

**Baselines.** We compare DETReg to several closely related state-of-the-art pretraining approaches for object detection with transformers: using a SwAV [6] backbone, a fully pre-

Method	PASCAL VOC			Airbus Ship		
	AP	AP <sub>50</sub>	AP <sub>75</sub>	AP	AP <sub>50</sub>	AP <sub>75</sub>
Supervised	59.5	82.6	65.6	79.8	95.8	89.4
SwAV [6]	61.0	83.0	68.1	78.3	95.7	88.7
<b>DETReg</b>	<b>63.5</b>	<b>83.3</b>	<b>70.3</b>	<b>81.0</b>	95.9	<b>89.7</b>

Table 2. **Object detection finetuned on PASCAL VOC and Airbus Ship data.** The model is finetuned on PASCAL VOC trainval07+2012 and evaluated on test07 (left), and Airbus Ship Detection finetuned on the train split and evaluated on the 3k test images (right). All models are based on Deformable DETR [71]. Bold values indicate an improvement  $\geq 0.3$  AP.

trained UP-DETR [16], and a supervised baseline backbone.

**Experiments.** To evaluate DETReg, we finetuned it on three different datasets: MS COCO [41], PASCAL VOC [18], and Airbus Ship Detection [1]. We perform an extensive comparison on MS COCO and finetune using similar training schedules as previously reported in [16, 71], using train2017 for finetuning and val2017 for evaluation. On PASCAL VOC and Airbus we use DETReg Deformable DETR based variant, which is faster to train. On PASCAL VOC we finetune on trainval07+12 for 100 epochs, dropping the learning rate after 70 epochs and use the test07 for evaluation. For Airbus, we finetune for 100 epochs, dropping the learning rate after 80 epochs.

**Results.** Table 1 shows that DETReg consistently outperforms other pretraining strategies using both DETR and Deformable DETR. For example, DETReg improves the COCO AP score by 1.4 points compared to UP-DETR when trained for 150 epochs, and in fact, outperforms the 300 epoch supervised variant after 150 epochs. Interestingly, using DETReg pretraining with DETR is competitive with supervised Deformable DETR, which achieves only 0.8 points (AP) more, despite significant architectural modifications.

Table 2 shows that DETReg improves by 2.5 (AP) points over SwAV on PASCAL VOC and by 1.2 (AP) on Airbus. For reference, by using a specialized architecture for ship detection that builds on a ResNet50 backbone, as well as leveraging the pixel-level annotations, [45] obtains a box AP score of 76.1 on this dataset, 4.9 points lower than DETReg, which only uses the bounding box annotations.

#### 4.2. Object Detection in Low-Data Regimes

These experiments test how DETReg performs when a small amount of annotated data is available for finetuning.

**Pretraining.** We pretrain DETReg based on Deformable DETR [71] for 5 epochs on ImageNet (IN1K).

**Baselines.** We consider recent approaches for pretraining ResNet50 backbone for object detection: InstLoc [67], ReSim [62] and SwAV [6], for each we use the publicly re-

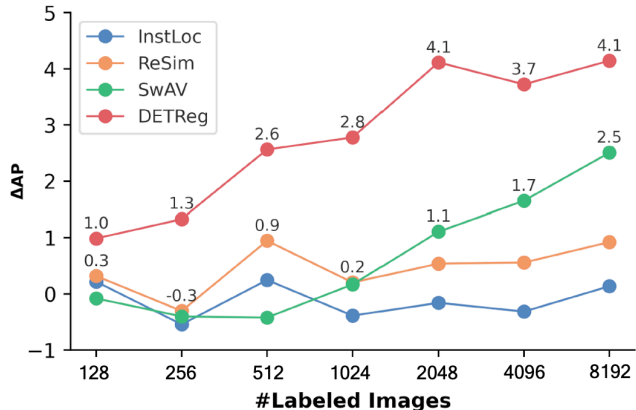


Figure 3. **Model comparison in low-data regimes.**  $\Delta AP$  improvement over the supervised baseline, where the x-axis shows the total number of images used during training. We fix the Deformable DETR architecture across all methods and finetuned it using publicly released ResNet50 weights of different methods on MS COCO `train2017` and evaluate on `val2017`.

leased checkpoint. We report the  $\Delta AP$  w.r.t. the supervised variant, which utilizes a ResNet50 pretrained on IN1K.

**Experiments.** We test the representations learned by DETReg when transferring with limited amounts of labeled data (up to 1024 labeled images), randomly sampled from MS COCO `train2017` and use `val2017` for evaluation. We train all methods for up to 2,000 epochs or until the validation performance stops improving.

**Results.** Figure 3 shows the results, where the y-axis reports the difference in AP compared to the supervised variant. The results indicate that DETReg consistently outperforms other pretraining strategies, when using Deformable DETR on low data regime. For example, when using only 256 images, DETReg improves the average precision (AP) score by 4.1 points compared to 1.1 for SwAV and 0.5 for ReSim.

### 4.3. Few-Shot Object Detection

These experiments test how DETReg extends to the few-shot settings established in existing literature.

**Pretraining.** We pretrain DETReg based on Deformable DETR [71] for 5 epochs on ImageNet (IN1K).

**Baselines.** We consider Deformable DETR with a supervised pretrained backbone as the most direct baseline as its architecture and training strategy mirror DETReg. We also report the results of recent few-shot approaches, which utilize different underlying object detectors. Concurrent to our work, Meta-DETR [69] proposed a new method based on Deformable DETR. However, unlike DETReg, it uses a ResNet101 backbone and a single image scale, but we include its results to encourage unified reporting, even when experimental settings are not perfectly aligned.

Model	Detector	Backbone	Novel AP 10	Novel AP 30	Novel AP <sub>75</sub> 10	Novel AP <sub>75</sub> 30
<i>Methods utilizing small backbones</i>						
YOLO-ft-full [35,47]	YOLOv2	DarkNet-19	3.1	1.7	7.7	6.4
FSRW [35]		DarkNet-19	5.6	9.1	4.6	7.6
FRCN-ft-full [66]	FRCN	VGG16	3.3	7.8	1.9	6.0
MetaDet [58]		VGG16	7.1	11.3	6.1	8.1
FRCN-ft-full [66]	FRCN	ResNet50	6.5	11.1	5.9	10.3
Meta R-CNN [66]		ResNet50	8.7	12.4	6.6	10.8
DDETR-ft-full	DDETR	ResNet50	12.4	20.4	13.3	21.8
<b>DETReg-ft-full</b>		ResNet50	<b>13.7</b>	<b>22.6</b>	<b>15.1</b>	<b>24.3</b>
<i>Methods utilizing large backbones</i>						
FRCN-ft-full [56]	FRCN	ResNet101	9.2	12.5	9.2	12.0
TFA [56]		ResNet101	10.0	13.7	9.3	13.4
DeFRCN [71]		ResNet101	18.5	<b>22.6</b>	-	-
DDETR-ft-full [69]	DDETR*	ResNet101	11.7	16.3	12.1	16.7
Meta-DETR [69]		ResNet101	<b>19.0</b>	22.2	<b>19.7</b>	22.8
<b>DETReg-ft-full</b>	DDETR	ResNet50	13.7	<b>22.6</b>	15.1	<b>24.3</b>

*DDETR\* is the customized single scale deformable DETR model used in [69].*

Table 3. **Few-shot detection evaluation on COCO.** We trained the model on the 60 base classes and then evaluate the model performance on the 20 novel categories, following the data split used in [56]. Through simple-fine tuning, DETReg outperforms previous few-shot object detectors with ResNet50 backbones. Using  $K = 30$ , DETReg achieves similar or improved performance compared to approaches that utilize larger backbones.

**Experiments.** Following the standard few-shot protocol for object detection [56], we finetune DETReg on the full data of 60 base classes, which contain around 99K labeled images. Then, we finetune on a balanced set of all 80 classes, where every class has  $k \in \{10, 30\}$  object instances. We use the splits from [56] and report the performance on the novel 20 classes. The results are shown in Table 3.

Table 4 shows an extreme few-shot setup where DETReg is finetuned on the balanced few-shot set without the intermediate finetuning on base classes. We consider finetuning the decoder only (*ft-decoder*) and the full model (*ft-full*).

**Results.** Table 3 shows that DETReg improves over supervised pretraining and achieves state-of-the-art 30-shot results compared to approaches that utilize larger backbones. DETReg only uses a simple fine-tuning strategy, while other methods may include more complicated episodic training.

Table 4 shows that DETReg achieves competitive few-shot performance even when the model is not trained on the abundant base class data. As a reference point, TFA [56] is a previous fine-tuning method that trains on the abundant base class data, and we can see that DETReg outperforms it without additional supervision from the base class data.

### 4.4. Semi-supervised Learning

These experiments test how DETReg compares to semi-supervised methods, where small amounts of labeled data and large amounts of unlabeled data are used during training. **Pretraining.** We pretrain DETReg (Deformable DETR) for

Model	Detector	Novel AP		Novel AP <sub>75</sub>	
		10	30	10	30
TFA [56] (w/base)	FRCN	10.0	13.7	9.3	13.4
DDETR-ft-full	DDETR	6.7	12.5	6.0	12.4
DDETR-ft-decoder		5.9	13.6	4.6	13.6
DETR-ft-decoder		7.6	15.7	7.7	16.6
<b>DETR-ft-full</b>		9.1	16.5	9.6	17.3

Table 4. **Few-shot object detection without training on the COCO base classes.** To test DETReg’s performance on extreme few-shot scenarios, we conduct an evaluation where DETReg is finetuned only on the  $K$ -shot COCO subsets. DETReg performs slightly worse ( $K = 10$ ) or better ( $K = 30$ ) compared to TFA [56] without using base class data while also using a smaller backbone.

Method	Detector	COCO			
		1%	2%	5%	10%
Supervised	DDETR	11.31 ± 0.3	15.22 ± 0.32	21.33 ± 0.2	26.34 ± 0.1
SwAV		11.79 ± 0.3	16.02 ± 0.4	22.81 ± 0.3	27.79 ± 0.2
ReSim		11.07 ± 0.4	15.26 ± 0.26	21.48 ± 0.1	26.56 ± 0.3
<b>DETR</b>		<b>14.58 ± 0.3</b>	<b>18.69 ± 0.2</b>	<b>24.80 ± 0.2</b>	<b>29.12 ± 0.2</b>

Table 5. **Object detection using  $k\%$  of the labeled data on COCO.** The models are trained on `train2017` using  $k\%$  and then evaluated on `val2017`.

50 epochs on MS COCO *train2017* without labels.

**Baselines.** We compare DETReg with a Deformable DETR model initialized with a supervised backbone from IN1K pre-training, which is the most direct baseline as all experiments are carried out on the same architecture and training data. We consider recent approaches for pretraining ResNet50 backbone for object detection like ReSim [62] and SwAV [6], for each we use the publicly released checkpoint.

**Experiments.** We finetuned DETReg on random  $k\%$  of `train2017` data for  $k \in \{1, 2, 5, 10\}$ , until convergence (validation performance stopped improving). In each setting, we train 5 different models with different random seeds and report the mean and standard deviation.

**Results.** Table 5 shows that DETReg outperforms existing pretraining methods, including a consistent improvement over the supervised pretraining baseline. We include a more broad comparison in the Supplementary Table 9, where we also compare to approaches that leverage both the labeled and unlabeled data via auxiliary losses [34, 42, 53, 65].

#### 4.5. DETReg Analysis

This section further explores and justifies the architectural and algorithmic choices used in the main experiments.

**Design Ablations.** Table 6 examines the contribution of the object localization and object embedding tasks in DETReg. To quantify the importance of using object-centric region proposals, we train DETReg while randomly shuffling

Proposals	$L_{emb}$	Frozen BB	$L_{class} \downarrow$	$L_{box} \downarrow$	AP
Shuffle	$\lambda_e = 0$		11.3	.044	32.0
Top-K	$\lambda_e = 0$		9.50	.037	43.3
Top-K	$\lambda_e = 1$		8.81	.037	45.1
Top-K	$\lambda_e = 2$		9.14	.039	43.8
Top-K	$\lambda_e = 1$	✓	<b>8.61</b>	<b>.037</b>	<b>45.4</b>

Table 6. **Ablation studies.** This tables ablates region proposal sampling strategies, values of  $\lambda_{emb}$ , and whether to freeze backbones with DETReg trained on *IN100* and finetuned on MS COCO. Shuffling the region proposals across images led to a 11.3 AP drop,  $L_{emb}$  has a consistent performance, and freezing the backbone does not significantly change the performance.

Method	AP	AP <sub>50</sub>	AP <sub>75</sub>	$R@1$	$R@10$	$R@100$
UP-DETR [16]	0.0	0.0	0.0	0.0	0.0	0.4
Rand. Prop.	0.0	0.0	0.0	0.0	0.0	0.8
Selective Search [54]	0.2	0.5	0.1	0.2	1.5	10.9
ImpSamp (ours)	0.7	2.0	0.1	0.3	1.8	9.0
Random-K (ours)	0.7	2.4	0.2	0.5	2.9	11.7
Top-K (ours)	<b>1.0</b>	<b>3.1</b>	<b>0.6</b>	<b>0.6</b>	<b>3.6</b>	<b>12.7</b>

Table 7. **Class agnostic object proposal evaluation on MS COCO `val2017`.** The models are trained on IN100 and for each method, we consider the top 100 proposals. We show DETReg identifies objects more effectively than the previous methods.

the proposal box locations across images, as indicated by “Shuffle” in the “Proposals” column. Second, to assess the contribution of the embedding loss  $L_{emb}$ , we evaluate DETReg with different coefficients  $\lambda_e \in \{0, 1, 2\}$ . Finally, we validate that performance does not drop when freezing the backbone during training, i.e. that the performance benefits stem from the core DETReg contributions. All models are trained on IN100 for 50 epochs and finetuned on MS COCO.

Table 6 justifies our design choices: shuffling the region proposals across images led to a 11.3 AP drop indicating that the object-centric proposal are important. We further see that the embedding loss  $L_{emb}$  has a relatively consistent performance improvements with changes of  $\leq 2$  AP for all setting, and we select  $\lambda_e = 1$  based on these results. Finally, the performance of DETReg with and without freezing the backbone encoder is relatively consistent with changes of 0.3 AP points between the two settings.

**Class Agnostic Object Detection.** We examine the class agnostic performance of DETReg variants discussed in Section 3, as well as region proposal and pretraining approaches. The results reported in Table 7 indicate that DETReg variants achieve improved performance over other pretraining approaches including solely using Selective Search. This indicates that coupling the object embedding and localization components in the DETReg model improves the localization ability. In addition, we observe that the Top-K region pro-

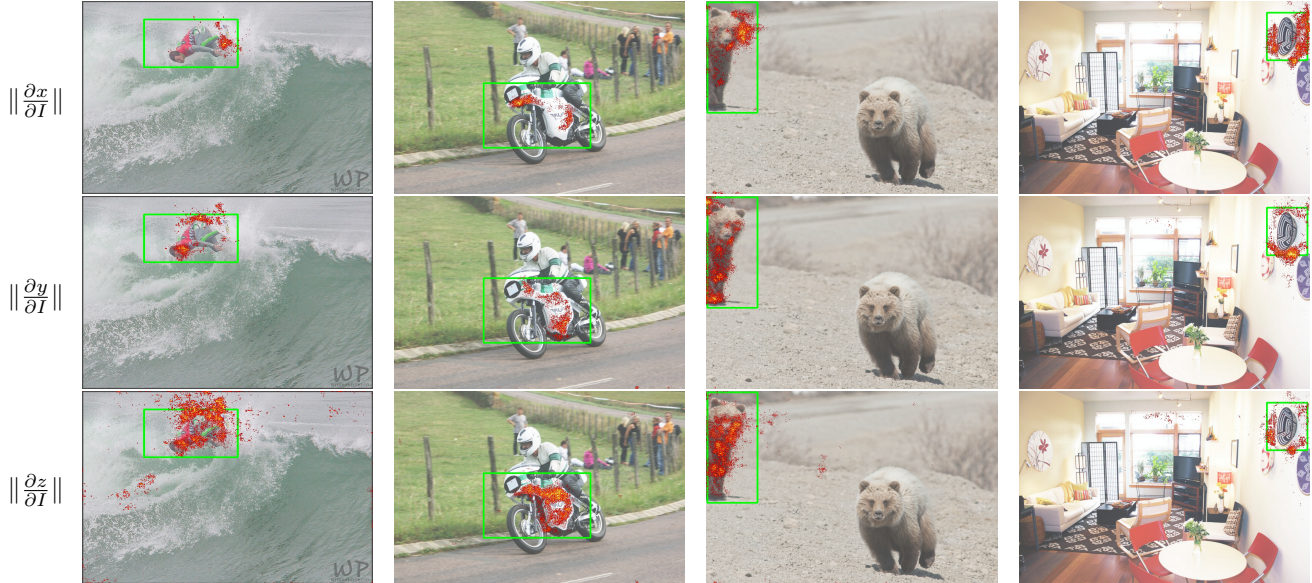


Figure 4. **DETReg visualization.** We show the gradient norms from the unsupervised DETReg detection with respect to the input image  $I$  for (top) the  $x$  coordinate of the object center, (middle) the  $y$  coordinate of the object center, (bottom) the feature-space embedding,  $z$ .

positional selection strategy performs best in these ablations.

**Robustness to different proposal methods.** We test how DETReg performs when pretrained with Selective Search proposals compared to Edge Box region proposals [72]. Specifically, we pretrain DETReg on IN100 and finetune on MS COCO with 2% and 10% of random data. We find that both variants perform similarly well with AP of 21.8 vs. 21.0 for 2% and a similar result of 36.2 for 10%.

**Visualizing DETReg.** Figure 4 shows qualitative examples of DETReg unsupervised box predictions with Deformable DETR. Additionally, it shows the Saliency Map [52] of the  $x/y$  bounding box center and the object embedding with respect to the input image  $I$ . The first three columns show the attention focusing on the object edges for the  $x/y$  predictions and  $z$  for the predicted object embedding. The final column shows a case where the background plays a more important role than the object in the embedding. We believe this may be due to the CNN-based encoder focusing on the textures rather than the shapes in the region as discussed in [21], and we view further exploration of such characteristics as an intriguing direction for future work.

## 5. Limitations

DETReg’s localization pretraining task uses simple region proposal methods for class-agnostic bounding-box supervision [3, 14, 15, 54]. While Table 7 indicates that DETReg performance can improve beyond these methods, DETReg class-agnostic results remain far behind supervised counterparts. Furthermore, our experiments focused on DETR [5]-related architectures, but it may be possible that DETReg

applies to more traditional detection architectures, which we leave for future work to explore. Finally, while DETReg improves training time, transformer-based object detectors still require significant computational resources to train.

## 6. Conclusion

We presented DETReg, an unsupervised pretraining approach for object detection with transformers using region priors. Through extensive empirical study, we showed DETReg learns representations in the unsupervised pretraining stage that lead to improvements in downstream performance for two different transformer models across three different datasets and many settings. We believe unsupervised pretraining holds the potential for positive social impact, mainly because it can utilize unlabeled data and reduce the need for massive amounts of labeled data which can be very expensive for fields like Medical Imaging. We do not anticipate a negative impact specific to our approach, but as with any model, we recommend careful validation before deployment.

## Acknowledgements

We would like to thank Sayna Ebrahimi and Jitendra Malik for their helpful feedback. This project has received funding from the European Research Council (ERC) under the European Unions Horizon 2020 research and innovation programme (grant ERC HOLI 819080). Prof. Darrell’s group was supported in part by DoD including DARPA’s LwLL and/or SemaFor programs, as well as BAIR’s industrial alliance programs. This work was completed in partial fulfillment for the Ph.D degree of the first author.

## References

- [1] Airbus. airbus ship detection challenge. <https://www.kaggle.com/c/airbus-ship-detection>. Accessed: 2021-09-30. **2, 5**
- [2] Bogdan Alexe, Thomas Deselaers, and Vittorio Ferrari. What is an object? In *CVPR*. IEEE, 2010. **3**
- [3] Pablo Arbeláez, Jordi Pont-Tuset, Jonathan T Barron, Ferran Marques, and Jitendra Malik. Multiscale combinatorial grouping. In *CVPR*, 2014. **2, 3, 8**
- [4] G. Bradski. The OpenCV Library. *Dr. Dobb's Journal of Software Tools*, 2000. **3, 12**
- [5] Nicolas Carion, Francisco Massa, Gabriel Synnaeve, Nicolas Usunier, Alexander Kirillov, and Sergey Zagoruyko. End-to-end object detection with transformers. *ECCV*, 2020. **2, 3, 4, 5, 8, 12, 13**
- [6] Mathilde Caron, Ishan Misra, Julien Mairal, Priya Goyal, Piotr Bojanowski, and Armand Joulin. Unsupervised learning of visual features by contrasting cluster assignments. *NeurIPS*, 2020. **1, 2, 4, 5, 7, 12**
- [7] Mathilde Caron, Hugo Touvron, Ishan Misra, Hervé Jégou, Julien Mairal, Piotr Bojanowski, and Armand Joulin. Emerging properties in self-supervised vision transformers. *arXiv preprint arXiv:2104.14294*, 2021. **4**
- [8] Joao Carreira and Cristian Sminchisescu. Cpmc: Automatic object segmentation using constrained parametric min-cuts. *TPAMI*, 34(7):1312–1328, 2011. **3**
- [9] Hao Chen, Yali Wang, Guoyou Wang, and Yu Qiao. Lstd: A low-shot transfer detector for object detection. In *Proceedings of the AAAI conference on artificial intelligence*, volume 32, 2018. **2**
- [10] Ting Chen, Simon Kornblith, Mohammad Norouzi, and Geoffrey Hinton. A simple framework for contrastive learning of visual representations. *arXiv preprint arXiv:2002.05709*, 2020. **2, 5, 12**
- [11] Ting Chen, Simon Kornblith, Kevin Swersky, Mohammad Norouzi, and Geoffrey Hinton. Big self-supervised models are strong semi-supervised learners. *NeurIPS*, 2020. **1**
- [12] Tung-I Chen, Yueh-Cheng Liu, Hung-Ting Su, Yu-Cheng Chang, Yu-Hsiang Lin, Jia-Fong Yeh, and Winston H Hsu. Should i look at the head or the tail? dual-awareness attention for few-shot object detection. *arXiv preprint arXiv:2102.12152*, 2021. **2**
- [13] Xinlei Chen, Haoqi Fan, Ross Girshick, and Kaiming He. Improved baselines with momentum contrastive learning. *arXiv preprint arXiv:2003.04297*, 2020. **2, 12**
- [14] Ming-Ming Cheng, Niloy J Mitra, Xiaolei Huang, Philip HS Torr, and Shi-Min Hu. Global contrast based salient region detection. *IEEE transactions on pattern analysis and machine intelligence*, 37(3):569–582, 2014. **2, 3, 8**
- [15] Ming-Ming Cheng, Ziming Zhang, Wen-Yan Lin, and Philip Torr. Bing: Binarized normed gradients for objectness estimation at 300fps. In *Proceedings of the IEEE conference on computer vision and pattern recognition*, pages 3286–3293, 2014. **2, 3, 8**
- [16] Zhigang Dai, Bolun Cai, Yugeng Lin, and Junying Chen. UP-DETR: Unsupervised pre-training for object detection with transformers. *CVPR*, 2021. **1, 3, 5, 7, 12**
- [17] Ian Endres and Derek Hoiem. Category-independent object proposals with diverse ranking. *TPAMI*, 36(2):222–234, 2013. **3**
- [18] Mark Everingham, Luc Van Gool, Christopher KI Williams, John Winn, and Andrew Zisserman. The pascal visual object classes (voc) challenge. *IJCV*, 88(2):303–338, 2010. **2, 5**
- [19] Qi Fan, Wei Zhuo, Chi-Keung Tang, and Yu-Wing Tai. Few-shot object detection with attention-rpn and multi-relation detector. In *Proceedings of the IEEE/CVF Conference on Computer Vision and Pattern Recognition*, pages 4013–4022, 2020. **2**
- [20] Zhibo Fan, Yuchen Ma, Zeming Li, and Jian Sun. Generalized few-shot object detection without forgetting. In *Proceedings of the IEEE/CVF Conference on Computer Vision and Pattern Recognition*, pages 4527–4536, 2021. **2**
- [21] Robert Geirhos, Patricia Rubisch, Claudio Michaelis, Matthias Bethge, Felix A Wichmann, and Wieland Brendel. Imagenet-trained cnns are biased towards texture; increasing shape bias improves accuracy and robustness. *arXiv preprint arXiv:1811.12231*, 2018. **8**
- [22] Spyros Gidaris, Andrei Bursuc, Nikos Komodakis, Patrick Pérez, and Matthieu Cord. Learning representations by predicting bags of visual words. In *CVPR*, 2020. **2, 12**
- [23] Ross Girshick. Fast r-cnn. In *ICCV*, 2015. **3**
- [24] Ross Girshick, Jeff Donahue, Trevor Darrell, and Jitendra Malik. Rich feature hierarchies for accurate object detection and semantic segmentation. In *CVPR*, 2014. **3**
- [25] Priya Goyal, Dhruv Mahajan, Abhinav Gupta, and Ishan Misra. Scaling and benchmarking self-supervised visual representation learning. In *ICCV*, 2019. **2, 12**
- [26] Jean-Bastien Grill, Florian Strub, Florent Altché, Corentin Tallec, Pierre Richemond, Elena Buchatskaya, Carl Doersch, Bernardo Avila Pires, Zhaohan Guo, Mohammad Gheshlaghi Azar, et al. Bootstrap your own latent—a new approach to self-supervised learning. *NeurIPS*, 2020. **1, 4**
- [27] Kaiming He, Haoqi Fan, Yuxin Wu, Saining Xie, and Ross Girshick. Momentum contrast for unsupervised visual representation learning. In *CVPR*, 2020. **1, 2, 5**
- [28] Kaiming He, Haoqi Fan, Yuxin Wu, Saining Xie, and Ross Girshick. Momentum contrast for unsupervised visual representation learning. In *CVPR*, 2020. **2, 5, 12**
- [29] Kaiming He, Ross Girshick, and Piotr Dollár. Rethinking imagenet pre-training. In *ICCV*, 2019. **2**
- [30] Kaiming He, Xiangyu Zhang, Shaoqing Ren, and Jian Sun. Deep residual learning for image recognition. In *CVPR*, 2016. **3**
- [31] Olivier J Hénaff, Skanda Koppula, Jean-Baptiste Alayrac, Aaron van den Oord, Oriol Vinyals, and João Carreira. Efficient visual pretraining with contrastive detection. *arXiv preprint arXiv:2103.10957*, 2021. **2**
- [32] Jan Hosang, Rodrigo Benenson, Piotr Dollár, and Bernt Schiele. What makes for effective detection proposals? *TPAMI*, 38(4):814–830, 2015. **3**
- [33] Jan Hosang, Rodrigo Benenson, and Bernt Schiele. How good are detection proposals, really? *arXiv preprint arXiv:1406.6962*, 2014. **3**

- [34] Jisoo Jeong, Seungeui Lee, Jeesoo Kim, and Nojun Kwak. Consistency-based semi-supervised learning for object detection. In *nips*, 2019. 2, 7, 12, 13
- [35] Bingyi Kang, Zhuang Liu, Xin Wang, Fisher Yu, Jiashi Feng, and Trevor Darrell. Few-shot object detection via feature reweighting. In *ICCV*, 2019. 2, 6
- [36] Leonid Karlinsky, Joseph Shtok, Sivan Harary, Eli Schwartz, Amit Aides, Rogerio Feris, Raja Giryes, and Alex M Bronstein. Repmet: Representative-based metric learning for classification and few-shot object detection. In *Proceedings of the IEEE/CVF Conference on Computer Vision and Pattern Recognition*, pages 5197–5206, 2019. 2
- [37] Philipp Krähenbühl and Vladlen Koltun. Geodesic object proposals. In *ECCV*, pages 725–739. Springer, 2014. 3
- [38] Harold W Kuhn. The hungarian method for the assignment problem. *Naval research logistics quarterly*, 2(1-2):83–97, 1955. 4
- [39] Aoxue Li and Zhenguo Li. Transformation invariant few-shot object detection. In *Proceedings of the IEEE/CVF Conference on Computer Vision and Pattern Recognition*, pages 3094–3102, 2021. 2
- [40] Tsung-Yi Lin, Priya Goyal, Ross Girshick, Kaiming He, and Piotr Dollár. Focal loss for dense object detection. In *ICCV*, 2017. 4
- [41] Tsung-Yi Lin, Michael Maire, Serge Belongie, James Hays, Pietro Perona, Deva Ramanan, Piotr Dollár, and C Lawrence Zitnick. Microsoft coco: Common objects in context. In *ECCV*. Springer, 2014. 2, 5
- [42] Yen-Cheng Liu, Chih-Yao Ma, Zijian He, Chia-Wen Kuo, Kan Chen, Peizhao Zhang, Bichen Wu, Zsolt Kira, and Peter Vajda. Unbiased teacher for semi-supervised object detection. *arXiv preprint arXiv:2102.09480*, 2021. 2, 7, 12, 13
- [43] Ishan Misra and Laurens van der Maaten. Self-supervised learning of pretext-invariant representations. In *CVPR*, 2020. 2, 12
- [44] Vinod Nair and Geoffrey E Hinton. Rectified linear units improve restricted boltzmann machines. In *ICML*, 2010. 4, 12
- [45] Xuan Nie, Mengyang Duan, Haoxuan Ding, Bingliang Hu, and Edward K Wong. Attention mask r-cnn for ship detection and segmentation from remote sensing images. *IEEE Access*, 8:9325–9334, 2020. 5
- [46] Saba Rahimi, Ozan Oktay, Javier Alvarez-Valle, and Sujeeth Bharadwaj. Addressing the exorbitant cost of labeling medical images with active learning. In *International Conference on Machine Learning in Medical Imaging and Analysis*, June 2021. Best Presentation Award. 1
- [47] Joseph Redmon and Ali Farhadi. Yolo9000: better, faster, stronger. In *Proceedings of the IEEE conference on computer vision and pattern recognition*, pages 7263–7271, 2017. 6
- [48] Colorado J Reed, Xiangyu Yue, Ani Nrusimha, Sayna Ebrahimi, Vivek Vijaykumar, Richard Mao, Bo Li, Shanghang Zhang, Devin Guillory, Sean Metzger, et al. Self-supervised pretraining improves self-supervised pretraining. *arXiv preprint arXiv:2103.12718*, 2021. 2
- [49] Shaoqing Ren, Kaiming He, Ross Girshick, and Jian Sun. Faster r-cnn: Towards real-time object detection with region proposal networks. In *NeurIPS*, 2015. 12
- [50] Hamid Rezaatofghi, Nathan Tsoi, JunYoung Gwak, Amir Sadeghian, Ian Reid, and Silvio Savarese. Generalized intersection over union: A metric and a loss for bounding box regression. In *CVPR*, 2019. 4
- [51] Byungseok Roh, Wuhyun Shin, Ildoo Kim, and Sungwoong Kim. Spatially consistent representation learning. *arXiv preprint arXiv:2103.06122*, 2021. 2
- [52] Karen Simonyan, Andrea Vedaldi, and Andrew Zisserman. Deep inside convolutional networks: Visualising image classification models and saliency maps. *arXiv preprint arXiv:1312.6034*, 2013. 8
- [53] Kihyuk Sohn, Zizhao Zhang, Chun-Liang Li, Han Zhang, Chen-Yu Lee, and Tomas Pfister. A simple semi-supervised learning framework for object detection. *arXiv preprint arXiv:2005.04757*, 2020. 2, 7, 12, 13
- [54] Jasper RR Uijlings, Koen EA Van De Sande, Theo Gevers, and Arnold WM Smeulders. Selective search for object recognition. *IJCV*, 104(2):154–171, 2013. 2, 3, 7, 8
- [55] Koen EA Van de Sande, Jasper RR Uijlings, Theo Gevers, and Arnold WM Smeulders. Segmentation as selective search for object recognition. In *ICCV*. IEEE, 2011. 3
- [56] Xin Wang, Thomas E Huang, Trevor Darrell, Joseph E Gonzalez, and Fisher Yu. Frustratingly simple few-shot object detection. *arXiv preprint arXiv:2003.06957*, 2020. 2, 6, 7
- [57] Xinlong Wang, Rufeng Zhang, Chunhua Shen, Tao Kong, and Lei Li. Dense contrastive learning for self-supervised visual pre-training. *arXiv preprint arXiv:2011.09157*, 2020. 12
- [58] Yu-Xiong Wang, Deva Ramanan, and Martial Hebert. Meta-learning to detect rare objects. In *Proceedings of the IEEE International Conference on Computer Vision*, pages 9925–9934, 2019. 6
- [59] Jiayi Wu, Songtao Liu, Di Huang, and Yunhong Wang. Multi-scale positive sample refinement for few-shot object detection. In *European Conference on Computer Vision*, pages 456–472. Springer, 2020. 2
- [60] Xiongwei Wu, Doyen Sahoo, and Steven Hoi. Meta-rcnn: Meta learning for few-shot object detection. In *Proceedings of the 28th ACM International Conference on Multimedia*, pages 1679–1687, 2020. 2
- [61] Zhirong Wu, Yuanjun Xiong, Stella X Yu, and Dahua Lin. Unsupervised feature learning via non-parametric instance discrimination. In *Proceedings of the IEEE Conference on Computer Vision and Pattern Recognition*, pages 3733–3742, 2018. 2, 12
- [62] Tete Xiao, Colorado J Reed, Xiaolong Wang, Kurt Keutzer, and Trevor Darrell. Region similarity representation learning. *arXiv preprint arXiv:2103.12902*, 2021. 1, 2, 5, 7, 12
- [63] Yang Xiao and Renaud Marlet. Few-shot object detection and viewpoint estimation for objects in the wild. In *European Conference on Computer Vision*, pages 192–210. Springer, 2020. 2
- [64] Enze Xie, Jian Ding, Wenhai Wang, Xiaohang Zhan, Hang Xu, Zhenguo Li, and Ping Luo. Detco: Unsupervised contrastive learning for object detection. *arXiv preprint arXiv:2102.04803*, 2021. 2, 5, 12
- [65] Mengde Xu, Zheng Zhang, Han Hu, Jianfeng Wang, Lijuan Wang, Fangyun Wei, Xiang Bai, and Zicheng Liu. End-to-

- end semi-supervised object detection with soft teacher. *arXiv preprint arXiv:2106.09018*, 2021. [2](#), [7](#), [12](#), [13](#)
- [66] Xiaopeng Yan, Ziliang Chen, Anni Xu, Xiaoxi Wang, Xiaodan Liang, and Liang Lin. Meta r-cnn: Towards general solver for instance-level low-shot learning. In *Proceedings of the IEEE International Conference on Computer Vision*, pages 9577–9586, 2019. [2](#), [6](#)
- [67] Ceyuan Yang, Zhirong Wu, Bolei Zhou, and Stephen Lin. Instance localization for self-supervised detection pretraining. In *CVPR*, 2021. [1](#), [5](#)
- [68] Jun Yu, Baopeng Zhang, Zhengzhong Kuang, Dan Lin, and Jianping Fan. iprivacy: image privacy protection by identifying sensitive objects via deep multi-task learning. *IEEE Transactions on Information Forensics and Security*, 12(5):1005–1016, 2016. [1](#)
- [69] Gongjie Zhang, Zhipeng Luo, Kaiwen Cui, and Shijian Lu. Meta-detr: Few-shot object detection via unified image-level meta-learning. *arXiv preprint arXiv:2103.11731*, 2021. [2](#), [6](#)
- [70] Dongzhan Zhou, Xinchu Zhou, Hongwen Zhang, Shuai Yi, and Wanli Ouyang. Cheaper pre-training lunch: An efficient paradigm for object detection. In *European Conference on Computer Vision*, pages 258–274. Springer, 2020. [2](#)
- [71] Xizhou Zhu, Weijie Su, Lewei Lu, Bin Li, Xiaogang Wang, and Jifeng Dai. Deformable DETR: Deformable transformers for end-to-end object detection. *arXiv preprint arXiv:2010.04159*, 2020. [2](#), [3](#), [4](#), [5](#), [6](#), [12](#)
- [72] C Lawrence Zitnick and Piotr Dollár. Edge boxes: Locating object proposals from edges. In *ECCV*. Springer, 2014. [3](#), [8](#)

## Supplementary Material

We start by providing the full implementation details of DETReg and include the complete PASCAL VOC results. We then follow with additional analysis of DETReg pretraining as well as class agnostic performance and visualization.

**Implementation Details.** Based on the ablations presented in Section 4.5, the default experiment settings are as follows. For region proposals, we compute Selective Search boxes online using the “fast” preset of the OpenCV implementation [4] and unless otherwise noted, we use the DETReg Top-K region selection variant (see Section 3.1) and set  $K = 30$  proposals per-image. We initialize the ResNet50 backbone of DETReg with SwAV [6], which was pretrained with multi-crop views for 800 epochs on IN1K, and fix it throughout the pretraining stage. A similar SwAV encoder is used to encode region proposals, which are first cropped and resized to  $128 \times 128$ . In the object embedding branch,  $f_{emb}$  and  $f_{box}$  are MLPs with 2 hidden layers of size 256 followed by a ReLU [44] nonlinearity. The output sizes of  $f_{emb}$  and  $f_{box}$  are 512 and 4.  $f_{cat}$  is implemented as a single fully-connected layer with 2 outputs. We run the pretraining experiments using a batch size of 24 per GPU on an NVIDIA DGX, V100 x8 GPUs machine, following the hyperparameter settings and image augmentations from existing works [5, 71]. Similarly, cropped regions are augmented before being fed to the encoder to obtain embeddings  $z_i$ . When finetuning, we drop the  $f_{emb}$  branch, and set the size of the last fully-connected layer of  $f_{cat}$  to be the number of classes in the target dataset plus a background class.

### Object Detection in Full Data Regimes

We reported DETReg results on the PASCAL VOC benchmark in Section 4.1. Here we include the full table, containing more past pretraining approaches using three different object detectors (see Table 8). We observe that using the Deformable-DETR detector, the supervised pretraining baseline is superior to past pretraining approaches and that DETReg pretraining improves over it by 4 points (AP).

### Semi-supervised Learning

We reported DETReg results and comparisons to other pretraining approaches like [6, 62] when using limited amounts of data. In Table 9, we include comparisons to semi-supervised works [34, 42, 53, 65] that leverage both the labeled and unlabeled data in training via auxiliary losses.

### DETReg Analysis

In Section 4.5 we analyzed DETReg, including the model ablations, class agnostic results, visualization and robustness. Here we further examine the pretrained DETReg model including the class agnostic results, and TopK selection policy.

Method	Detector	AP	AP <sub>50</sub>	AP <sub>75</sub>
Supervised	FRCN	56.1	82.6	62.7
InsDis [61]		55.2	80.9	61.2
Jigsaw [25]		48.9	75.1	52.9
NPID++ [43]		52.3	79.1	56.9
SimCLR [10]		51.5	79.4	55.6
PIRL [43]		54.0	80.7	59.7
BoWNet [22]		55.8	81.3	61.1
MoCo [28]		55.9	81.5	62.6
MoCo-v2 [13]		57.0	82.4	63.6
SwAV [6]		56.1	82.6	62.7
DenseCL [57]		58.7	82.8	65.2
DetCo [64]		58.2	82.7	65.0
ReSim [62]		59.2	82.9	65.9
Supervised	DETR	54.1	78.0	58.3
UP-DETR [16]		57.2	80.1	62.0
Supervised	DDETR	59.5	82.6	65.6
SwAV [6]		61.0	83.0	68.1
DETReg		<b>63.5</b>	<b>83.3</b>	<b>70.3</b>

Table 8. **Object detection finetuned on PASCAL VOC.** The model is finetuned on PASCAL VOC `trainval07+2012` and evaluated on `test07`. Models are based on Faster-RCNN [49] (FRCN), DETR [5], and Deformable DETR [71] (DDETR). Bold values indicate an improvement  $\geq 0.3$  AP.

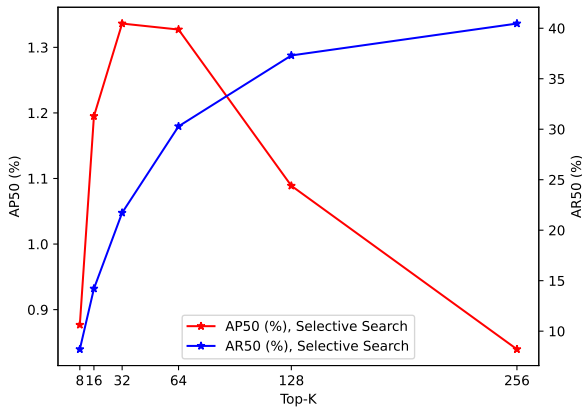


Figure 5. **Top-K proposals performance of Selective Search.** Using different values of  $K$ , we evaluate the class agnostic performance of Selective Search on MS COCO 2017 validation split.

**Improved Encoder, improved DETReg.** We test how DETReg performs when object embeddings are obtained with different image encoders. Specifically, we pretrain DETReg on IN100 using SwAV trained for 400 epochs compared to a superior variant trained for 800 epochs with multi-crops. We finetune on MS COCO with 1% data and observe the improved encoder achieves 1 AP improvement (27.7 vs 26.7).

**DETReg TopK selection policy.** Using Selective Search, we examine the class agnostic performance when using TopK

Method	Approach	Detector	COCO			
			1%	2%	5%	10%
CSD [34]	Auxiliary	FRCN	$10.5 \pm 0.1$	$13.9 \pm 0.1$	$18.6 \pm 0.1$	$22.5 \pm 0.1$
STAC [53]			$14.0 \pm 0.6$	$18.3 \pm 0.3$	$24.4 \pm 0.1$	$28.6 \pm 0.2$
U-T [42]			$20.8 \pm 0.1$	$24.3 \pm 0.1$	$28.3 \pm 0.1$	$31.5 \pm 0.1$
S-T [65]			<b><math>20.5 \pm 0.4</math></b>	–	<b><math>30.7 \pm 0.1</math></b>	<b><math>34.0 \pm 0.1</math></b>
Supervised	Pretraining	DDETR	$11.31 \pm 0.3$	$15.22 \pm 0.32$	$21.33 \pm 0.2$	$26.34 \pm 0.1$
SwAV			$11.79 \pm 0.3$	$16.02 \pm 0.4$	$22.81 \pm 0.3$	$27.79 \pm 0.2$
ReSim			$11.07 \pm 0.4$	$15.26 \pm 0.26$	$21.48 \pm 0.1$	$26.56 \pm 0.3$
<b>DETReg</b>			<b><math>14.58 \pm 0.3</math></b>	<b><math>18.69 \pm 0.2</math></b>	<b><math>24.80 \pm 0.2</math></b>	<b><math>29.12 \pm 0.2</math></b>

Table 9. **Object detection using k% of the labeled data on COCO.** The models are trained on `train2017` using k% and then evaluated on `val2017`. Methods like [42] utilize auxiliary losses during the training stage using unlabeled data, whereas DETReg utilizes unlabeled data during the pretraining stage only.

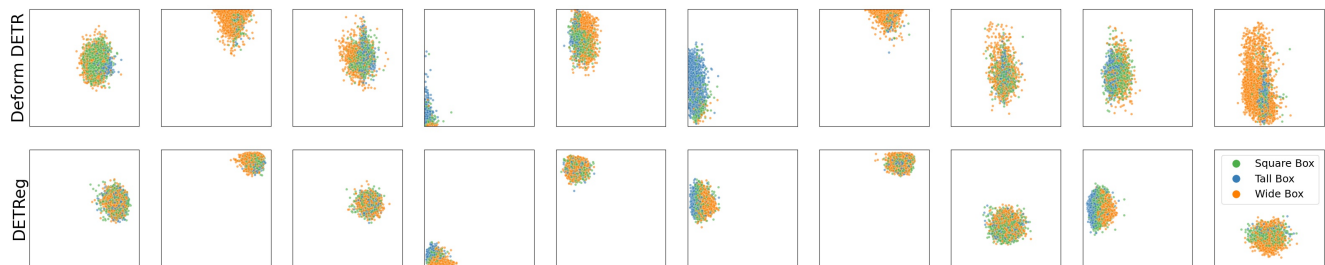


Figure 6. **DETReg slots specialize in specific areas in the image and uses a variety of box sizes much like Deformable DETR.** Each square corresponds to a DETR slot, and shows the location of its bounding box predictions. We compare 10 random slots of the supervised Deformable DETR (**top**) and unsupervised DETReg (**bottom**) decoder for the MS COCO 2017 val dataset. Each point shows the center coordinate of the predicted bounding box, where following a similar plot in [5], a **green point** represents a square bounding box, a **orange point** is a large horizontal bounding box, and a **blue point** is a large vertical bounding box. Deformable DETR has been trained on MS COCO 2017 data, while DETReg has only been trained on unlabeled ImageNet data. Similar DETReg and Deformable DETR slots were manually chosen for illustration.

policy. We report the precision and recall in Figure 5. In this paper, we have used  $K = 30$  (see Figure 7), which emphasizes precision over recall. This might imply that DETReg performs well given high precision proposals.

**DETReg Slots Visualization.** We examine the learned object queries slots (see Figure 6) and observe they are similar to those in Deformable DETR, despite not using any human annotated data. Nevertheless, the Deformable DETR slots

have greater variance with respect to locations and they tend to specialize more in particular boxes shapes.

**Class Agnostic Object Detection.** The quantitative results in Section 4.5 indicate that DETReg improves over Selective Search. The included qualitative examples of DETReg on MS COCO (see Figure 8) supports a similar conclusion, indicating that DETReg outperforms Selective Search but still much behind the ground truth labeled data.

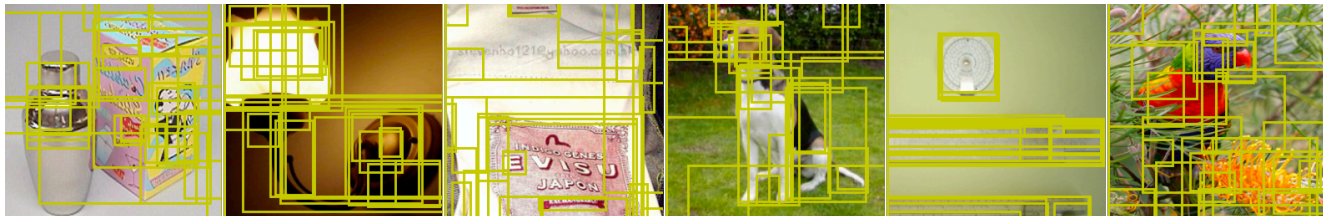


Figure 7. **TopK Selective Search proposals on ImageNet.** Using  $K=30$ , the proposals typically cover objects and parts-of-objects in the image.

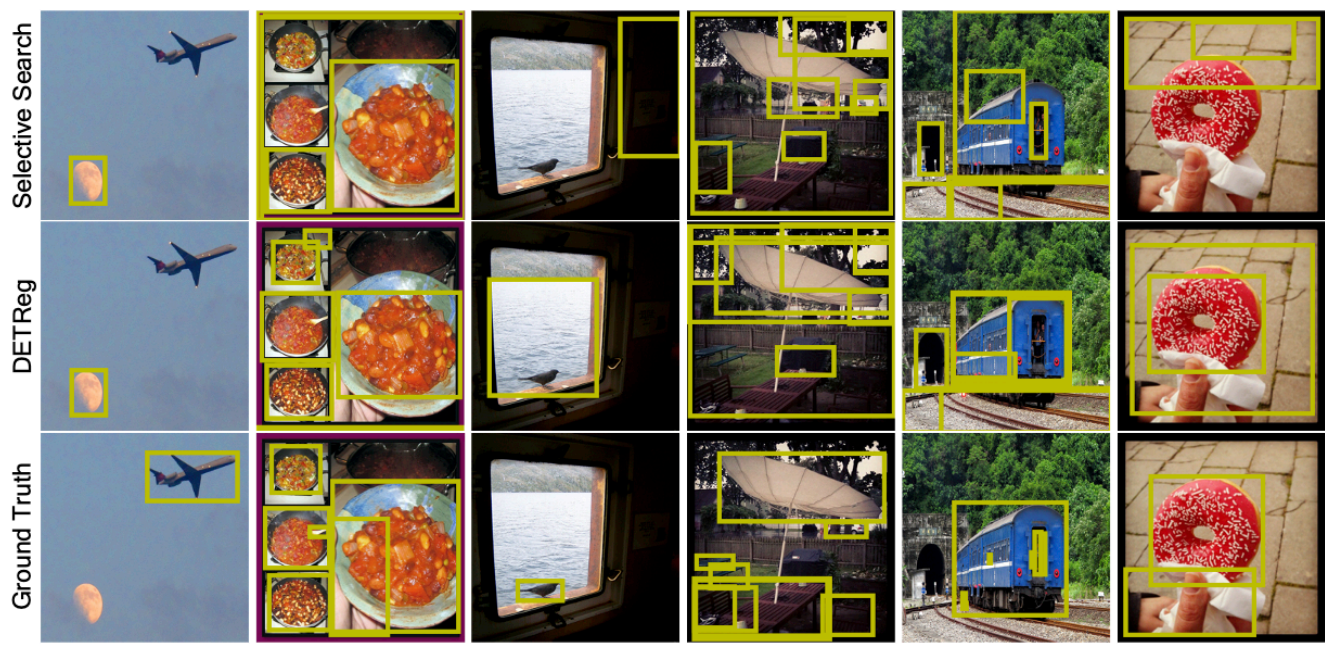


Figure 8. **Class Agnostic object detection visualization.** Examples predictions using Selective Search and DETReg on random MS COCO images. For every image annotated with  $M$  boxes, only the top  $M$  predictions are shown.